

Prebiotic Chemistry

Thermal Behavior of D-Ribose Adsorbed on Silica: Effect of Inorganic Salt Coadsorption and Significance for Prebiotic Chemistry

Mariame Akouche,^[a] Maguy Jaber,^[b] Emilie-Laure Zins,^[c] Marie-Christine Maurel,^[d] Jean-Francois Lambert,^{*[a]} and Thomas Georgelin^{*[a]}

Abstract: Understanding ribose reactivity is a crucial step in the "RNA world" scenario because this molecule is a component of all extant nucleotides that make up RNA. In solution, ribose is unstable and susceptible to thermal destruction. We examined how ribose behaves upon thermal activation when adsorbed on silica, either alone or with the coadsorption of inorganic salts (MgCl₂, CaCl₂, SrCl₂, CuCl₂, FeCl₂, FeCl₃, ZnCl₂). A combination of ¹³C NMR, in situ IR, and TGA analyses revealed a variety of phenomena. When adsorbed alone, ribose remains stable up to 150 °C, at which point ring opening is observed, together with minor oxidation to a lactone. All the metal salts studied showed specific interactions with ribose after dehydration, resulting in the formation of poly-

dentate metal ion complexes. Anomeric equilibria were affected, generally favoring ribofuranoses. Zn²⁺ stabilized ribose up to higher temperatures than bare silica (180 to 200 °C). Most other cations had an adverse effect on ribose stability, with ring opening already upon drying at 70 °C. In addition, alkaline earth cations catalyzed the dehydration of ribose to furfural and, to variable degrees, its further decarbonylation to furan. Transition-metal ions with open d-shells took part in redox reactions with ribose, either as reagents or as catalysts. These results allow the likelihood of prebiotic chemistry scenarios to be evaluated, and may also be of interest for the valorization of biomass-derived carbohydrates by heterogeneous catalysis.

Introduction

In the prebiotic scenario of the "RNA world",^[1] RNA oligomers are considered as the first biological molecules to have emerged. This idea is based on the fact that some RNAs are the only biopolymers to possess both information capability and catalytic properties, which are currently observed in several ribozymic motifs and species such as viroids. Combining both abilities in the same molecule eschews the "chicken-and-egg" dilemma that would be implied if the choice were between DNA and proteins.

RNA is a polymer of nucleotides, themselves composed of phosphates, nucleobases and a specific pentose carbohydrate, namely D-ribose. Therefore, studies of ribose synthesis, of its conditions of stability, and of its further reactions such as phosphorylation and glycosylation are particularly interesting to explain the formation of RNA.

Ribose can be synthesized under abiotic conditions together with other carbohydrates from the formose reaction,^[2] based on the polymerization of formaldehyde; in particular, its synthesis has been reported in analogues of interstellar ices.^[3] Once ribose is formed, several pathways could lead to nucleosides, and recent investigations have shown good yields and selectivities.^[4] Yet these scenarios are plagued by several problems. First, ribose is often a rather minor product of the formose reaction.^[5] Second, assuming it can be synthesized, the ribose molecule is quite unstable in aqueous solution.^[6] For example, at pH 9 and 60 °C, its half-life is about 50 h; closer to physiological conditions, at pH 7 and 37 °C, it should be around 500 h if one extrapolates from the data of Miller and co-workers.^[6] Then, as in many prebiotic scenarios, there is a selectivity problem. Not only does life use only D-ribose, excluding L-ribose, but among the four anomeric forms of this molecule (cf. Scheme 1), nucleotides and RNA exclusively use the β-D-ribofuranose form. In aqueous solutions, in contrast, this form is not predominant, typically accounting for 12% of all ribose in solution.^[7]

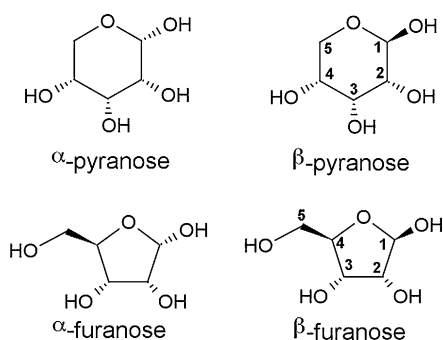
[a] M. Akouche, J.-F. Lambert, T. Georgelin
Sorbonne Universités, UPMC Univ Paris 06 and CNRS UMR 7197, LRS case courrier 178, UPMC 4 Pl. Jussieu, 75252 PARIS CEDEX 05 (France)
E-mail: thomas.georgelin@upmc.fr
jean-francois.lambert@upmc.fr

[b] M. Jaber
Sorbonne Universités, UPMC Univ Paris 06 and CNRS UMR 8220, LAMS, case courrier 225, UPMC 4 Pl. Jussieu, 75252 Paris CEDEX 05 (France)

[c] E.-L. Zins
Sorbonne Universités, UPMC Univ Paris 06 and CNRS UMR 8233, MONARIS, case courrier, UPMC 4 Pl. Jussieu, 75252 Paris CEDEX 05 (France)

[d] M.-C. Maurel
UMR 7205- ISyEB, CNRS-MNHN-UPMC Univ Paris 06, 75005 Paris (France)

Supporting information for this article is available on the WWW under <http://dx.doi.org/10.1002/chem.201601418>. It contains further experimental details (tables and figures).



Scheme 1. Ribose polymorphs.

Recent studies have attempted to solve the stability and the selectivity problems by invoking the formation of borate or silicate complexes in solution.^[2,8] These complexes result from the formation of two covalent bonds between the oxygen atoms of two -OH groups of the ribose molecule and the boron (resp. silicon) atom. It has been observed that such a complexation stabilizes ribose, and furthermore, preferably its furanose forms. Theoretical results have shown that indeed silicate/ribose complexes should be formed exclusively with the furanose form, because its HO-C-C-OH dihedral angle is sufficiently small to allow the formation of a planar five-membered ring.^[8c]

The silicate or borate scenarios have shown the potential of considering inorganic/organic interactions to study the origins of life. They deal with interactions in solution; another direction of research is the interaction of small biological molecules with surfaces of inorganic materials, i.e., interfacial chemistry. It was first proposed in 1951^[9] that mineral surfaces could have played a role in the emergence of life. Later, experimental studies showed that, for example, silica and clay surfaces can indeed induce prebiotically interesting reactions such as the formation of peptide bonds between amino acids,^[10] which is related to the capacity for protein adsorption,^[11] or the oligomerization of nucleotides.^[12] Our team has demonstrated the ability of silica and other surfaces to promote the oligomerization of amino acids to peptides or of monophosphate to polyphosphates.^[13] We have also recently reported that the silica surface stabilizes D-ribose upon drying, and causes a small but significant selection of the furanose form.^[14]

The present work intends to expand these initial results by focusing on the thermal reactivity of ribose adsorbed on amorphous silica (SiO₂). Silica represents a realistic model of mineral phases existing on the primitive earth such as cherts; it is also a desirable support from the point of view of the ease of characterization by such techniques as IR, NMR, and TGA.^[13h] Our goal is to study ribose reactions of prebiotic interest such as glycosylation or phosphorylation on the surface of silica. The study of the thermal reactivity of ribose is a prerequisite for such studies because the reagents should not be destroyed under the conditions tested.

To our knowledge, there is no information about the thermal reactivity of pentoses adsorbed on mineral surfaces. There exist some studies on the thermal reactivity of bulk carbohy-

drates^[15] but even in this case many questions remain unanswered because these studies are often concerned only with applications to the analysis of carbohydrate mixtures. Studies of sugars in acidic solutions or brines are also relevant because they illustrate some of the possible reactions of carbohydrates, from ring opening to the formation of furfural by dehydration when the activity of water is low enough. Lactones (cyclic esters) can also be formed but they require an oxidative step: the sugar ring is opened and isomerized to the enediol form, and the latter is oxidized to a linear carboxylic acid, which produces the lactone by internal condensation with recyclicalization.

In the present study we evaluate the stability of ribose under thermal activation and analyze the chemical behavior of ribose on silica surfaces, both alone and in the presence of inorganic salts. In a prebiotic setting, the deposition of ribose from an aquifer, presumably upon drying, could have been accompanied by the co-deposition of minerals from sea water. We chose not to attempt to reproduce a realistic composition of primordial seawater, but to focus on simple systems consisting of ribose and the chloride salt of Mg²⁺, Ca²⁺, Sr²⁺, Fe²⁺, Fe³⁺, Cu²⁺, and Zn²⁺. Mg²⁺ is well-known for its role in the coordination chemistry of nucleotides. Compared with the other alkaline earth cations (Ca²⁺ and Sr²⁺), Mg²⁺ can provide information on the role of Lewis acidity, which increases when going up the alkaline earth column in the periodic table. Furthermore, Mg²⁺ and Ca²⁺ easily leach from meteoritic minerals.^[16] The other four elements are transition metals that could have leached from the prebiotically important sulfide minerals.^[17] Fe²⁺, Fe³⁺, and Cu²⁺ have open (nd) subshells, allowing them to take part in redox reactions.

Materials and Methods

Adsorption procedures

Ribose adsorption was carried out by impregnation methods. In this procedure, 300 mg of amorphous silica (380 m²g⁻¹) was wetted with 4 mL of a ribose solution. The ribose concentrations were chosen so as to provide 5.0, 10.0, and 15.0 weight% ribose loading with respect to the silica support. The pastes obtained after wetting of the silica were stirred at room temperature for 3 h and then dried overnight at 70 °C in an oven under room humidity. Samples obtained after drying will be denoted as 5% ribose/SiO₂, etc. "ribose/SiO₂", with the percentage value omitted, will refer to the "basis" sample, that is, to the 10% loading.

Experiments were also carried out in which ribose was coadsorbed with divalent metal salts. 10.0 weight% of ribose per silica weight were coadsorbed with metal chloride, using ribose/metal molar ratios of either 1:1 or 2:1. The samples were equilibrated and dried in the same way as for the ribose/SiO₂ series. Dried samples will be called ribose-metal (x:1)/SiO₂; when the molar ratio is omitted, it is understood to be equal to (1:1).

Analytical techniques

X-ray powder diffraction (XRD) was carried out with a Bruker D8 Avance diffractometer using $\text{CuK}\alpha$ radiation (wavelength $\lambda = 1.5404 \text{ \AA}$). XRD patterns were recorded between 3° and 70° with a step size of 0.05° .

TGA of the samples was carried out with a TA Instruments Waters LLC, with a SDT Q600 analyzer, using a heating rate $\beta = 5^\circ\text{Cmin}^{-1}$ under dry air flow (100 mLmin^{-1}). For silica-supported samples, masses were normalized to the residual mass at 800°C , which corresponds to anhydrous silica without organic matter. All the weight losses assigned to transformations of supported organic molecules were quantified between limits determined from the DTG traces, and corrected for the weight loss of the bare support in the same temperature range.

Infrared (IR) spectra of solid samples were recorded in the transmission mode on self-supported pellets in a cell fitted with KBr windows. Samples may have two positions in the cell; one position is in the oven, allowing in situ thermal treatment under vacuum or various atmospheres, and the second position allows room-temperature recording of spectra without re-exposure to air. Fourier-transform (FT) IR spectra were recorded with a Bruker-Vector 22 FTIR spectrometer equipped with a deuterated triglycine sulfate (DTGS) detector, having a nominal resolution of 4 cm^{-1} , by adding 128 scans.

Attenuated total reflectance Fourier-transform infrared spectroscopy (ATR-FTIR) was used complementarily to investigate the effect of the temperature on bulk ribose. For these experiments, the samples were heated inside a heat chamber at ambient pressure. For each sample, 40 scans were added and the spectra were registered in the $400\text{--}4000 \text{ cm}^{-1}$ spectral region with a nominal resolution of 1 cm^{-1} . The ATR-FTIR approach provides spectral information while minimizing sample preparation.

Solid-state ^{13}C cross-polarization magic angle spinning (CP-MAS) NMR spectra were recorded at room temperature with a Bruker Avance 500 spectrometer with a field of 11.7 T equipped with a 4 mm MAS probe with a spinning rate of 10 kHz. The pulse angle was 30° , decoupling was applied at 50 KHz, and the recycle time was 10 s for bulk ribose and 1 s for adsorbed ribose. The contact time was $1000 \mu\text{s}$ (other values were also tested in one instance, see below).

Liquid-state ^{13}C NMR spectra were recorded with a Bruker Avance III 500 spectrometer, using a 1D sequence with power-gated decoupling, a 30° flip angle and a recycle time of 2 s.

Results and Discussion

Thermal reactivity of bulk ribose

TGA

Figure 1 shows the DTG signals of the various samples heated under dry air flow. Bulk D -ribose shows an endothermic event without weight change at 90°C , due to ribose melting,^[15a] followed by four weight loss events at 195°C (endothermic, -20% of starting mass), 280°C and 320°C (both exothermic, -51%) and 510°C (strongly exothermic, -29%) finally result-

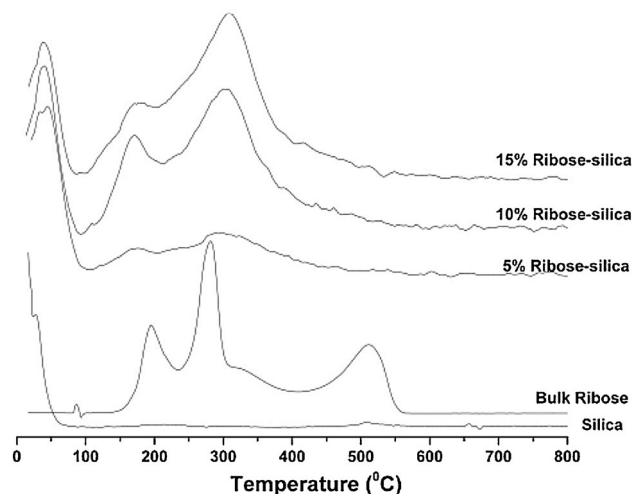


Figure 1. DTG traces of the silica support, of bulk ribose, and of samples 5% ribose/ SiO_2 , 10% ribose/ SiO_2 , and 15% ribose/ SiO_2 .

ing in quantitative combustion (Figure 1). No significant weight loss was observed before 195°C , but already after melting, liquid ribose shows signs of transformation such as browning and a typical lactone odor. In addition, as the following paragraph shows, tautomerization reactions are suggested by IR, which cannot be detected by TG because they do not cause any weight loss. This behavior is compatible with the rather limited information available in the literature on the TG of pentoses.^[18] The endothermic event at 195°C could be due to a dehydration step (the corresponding weight loss amounts to between one and two water molecules per ribose unit). It has been claimed to be indicative of carbohydrate polymerization by condensation, but the matter has not been investigated in detail. The material collected after this step was black and vitreous. Full polymerization to infinite chains would result in the elimination of only one water molecule per ribose, so the larger values measured indicate that modifications of the ribose skeleton also occur in the 195°C event.

FTIR spectroscopy

The IR spectra of bulk D -ribose were recorded at increasing temperatures, below and above the melting point (Figure 2 A: rapid heating, and 2B: slow heating). At room temperature, the spectrum presents vibrational bands characteristic of cyclic ribose. Table SI-1 shows that our data are in good agreement with those previously published by Mathlouthi and Seuvre.^[19] Some of the proposed assignments are open to question; in particular, these authors have claimed to observe vibrations attributable to both the pyranose form (1116 cm^{-1} , 890 cm^{-1}) and the furanose form (1160 cm^{-1} , 910 cm^{-1}), which seems at odds with solid-state NMR results (see below). In fact, we carried out numerical calculations suggesting that it is extremely difficult to discriminate the different anomers based on their vibrational frequencies. These data will be the object of a later publication. For the time being, we may underline that the most intense vibrations of D -ribose fall between 1200 and

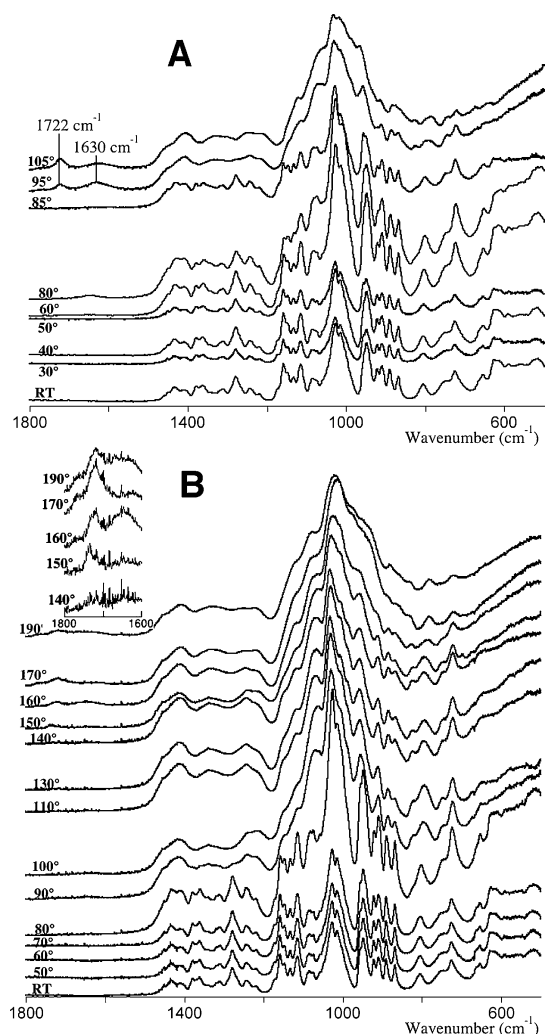
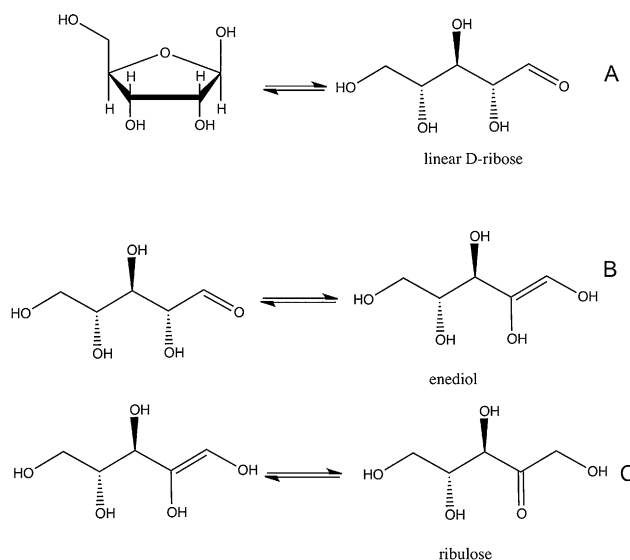


Figure 2. Influence of heating under air on IR-ATR of bulk *D*-ribose. A) rapid heating of 0.1 mg of *D*-ribose; B) progressive heating of 5 mg of *D*-ribose.

900 cm^{-1} , which will later preclude their observation in ribose/ SiO_2 samples because of overlap with the lattice vibrations of the SiO_2 support. At room temperature, no carbonyl signal was present, meaning there was no linear ribose (or products of further degradation, cf. infra).

Two series of spectroscopic experiments were carried out to investigate the thermal processes occurring in this crystalline sample. In the first series of experiments, 0.1 mg of *D*-ribose was subjected to rapid heating by using a heatgun. In the second series of experiments, 5.0 mg of *D*-ribose was progressively heated inside a heating chamber.

For quick heating, as long as the sample remained below the melting point, no structural evolution was observed. More specifically, no vibrational bands were observed in the carbonyl region. Above the melting point (90°C), two vibrational bands appeared at 1722 cm^{-1} ($\nu\text{C=O}$) and 1630 cm^{-1} (δOH ; Figure 2 A). They are respectively diagnostic of linear *D*-ribose and the enediol species.^[20] This means that in bulk liquid ribose, thermal activation has caused the opening of the ribose ring and that a keto-enol isomerization has taken place (Scheme 2), similar to the reactivity of ribose in solution.



Scheme 2. Thermally-induced ring opening (A) and enolization (B) equilibria of *D*-ribose (with the β -furanose polymorph chosen as the starting point). Transformation of the enolic form into *D*-ribulose (C) is also illustrated.

Furthermore, the shapes of the bands between 1500 and 500 cm^{-1} are strongly affected by heating: below 85°C , well-resolved bands are observed whereas above the melting point, they are significantly broadened and an envelope is observed. This suggests a degree of chemical heterogeneity in the liquid.

In the second series of experiments in which a more gentle heating was applied to 5.0 mg of *D*-ribose (Figure 2 B), a similar trend was observed, but the linear *D*-ribose and the enediol species only appeared at higher temperatures (around 150°C instead of 90°C). Furthermore, the amounts of these two species appear to be more limited. We believe that polymerization is in competition with the ring-opening process, and is more favored under gentle heating, that is, in the second heating procedure for IR, but also in the TGA experiments.

Thermal reactivity of adsorbed ribose

X-Ray diffraction (XRD) and TGA

We estimate that a physical monolayer of ribose molecules on a surface would correspond to 1.6 molecules per nm^2 . This Figure can be compared to the surface densities of ribose in our samples, namely 0.5, 1.1, and 1.5 molecules per nm^2 for 5, 10, and 15% ribose/ SiO_2 respectively, suggesting submonolayer coverage (but close to the monolayer for 15% ribose/ SiO_2). Indeed no trace of bulk ribose was detected by XRD in any of these samples.

TGA of the silica support (Figure 1) shows that it undergoes a strongly endothermic loss of physisorbed water up to 100°C , followed by a continuous, low-intensity weight loss between 100 and 600°C , without clearly defined maxima, that can be assigned to the condensation of surface silanols.^[21]

Figure 1 also shows the differential thermograms (DTG) of 5.0, 10.0, and 15.0% ribose/ SiO_2 . As on the raw silica support, desorption of physisorbed water is observed between 20 and 110°C . Two broad events at 170 and 308°C are present only in

Table 1. Weight losses (in weight% of the silica support) corresponding to the two DTG peaks attributable to supported ribose.

Sample	Weight loss [%]		total
	1st peak	2nd peak	
5% ribose/SiO ₂	1.1	3.8	4.9
10% ribose/SiO ₂	2.5	7.3	9.8
15% ribose/SiO ₂	2.6	10.5	13.1

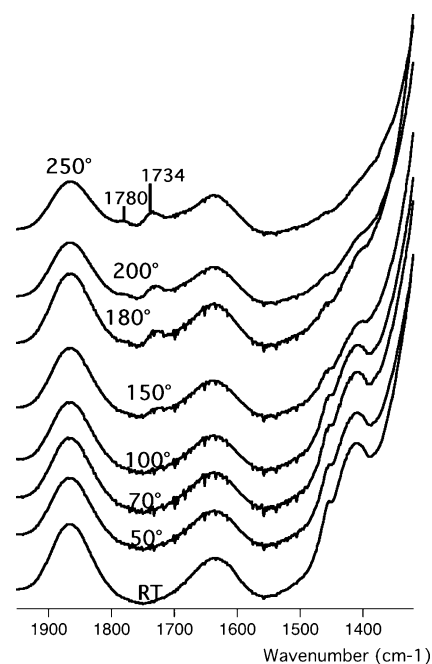
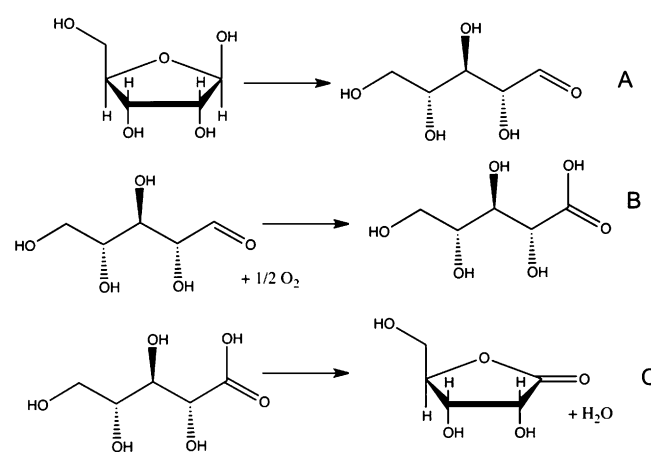
the ribose-containing samples; as shown in Table 1, the total weight loss for these two events (corrected for the contribution of the support) is close to the nominal ribose loading, and therefore most of the supported ribose has been eliminated by 450 °C.

The event at 170 °C is endothermic. The associated weight loss amounts to one to two molecules of water per ribose unit—in fact, close to two molecules for 5% and 10% ribose/SiO₂. The event at 308 °C is exothermic, probably corresponding to combustion of the remaining organic matter.

FTIR analyses were carried out on supported ribose samples. The spectra contain less usable information than those of bulk ribose because of the predominance of vibrational bands of silica. Only the region between 1900 and 1350 cm⁻¹ can be observed without interference from the silica bands. Our previous work^[14] showed that ribose is adsorbed on silica under its cyclic form and no trace of degraded products is observable at room temperature, as confirmed by the results of ¹³C NMR spectroscopic analysis. All the IR bands recorded at room temperature may be assigned to cyclic ribose and silica nanoparticles.

The IR spectrum of 10% ribose/SiO₂ is shown in Figure 3 (it may be compared with the spectra of 5 and 15% ribose/SiO₂ given in Figure SI-1). At room temperature, the observable bands (mostly the δ_{HCH} at 1455 and 1410 cm⁻¹) could be ascribed to adsorbed cyclic ribose, with no indication of degradation. Activation at temperatures lower than 150 °C did not result in any significant modification of the spectrum. From 150 to 180 °C, a vibrational band grew in the $\nu_{\text{C=O}}$ region, and as in the case of bulk ribose (cf. supra), it can probably be assigned to linear ribose; it seemed to shift as a function of temperature, because it was first centered at 1723 cm⁻¹ and moved to 1728 cm⁻¹ after activation at the final temperature of 250 °C. The shift of this band with respect to bulk ribose could be due to the isomerization to linear ribulose, which has been reported for ribose submitted to thermal activation in solution.^[20] The intermediate in the formation of this compound is the enediol form of ribose (cf. Scheme 2), which should have a characteristic vibration in the 1630–1650 cm⁻¹ range. No new signal was clearly observed in this region, but a small contribution would probably not be distinguished from the residual δ_{HOH} band of H₂O, and therefore we cannot exclude the presence of this intermediate.

From 180 to 250 °C, a second vibrational band appears at 1775 cm⁻¹, which could be attributed to a cyclic ester such as that present in ribonolactone.^[22] The formation of ribonolactone from ribose is an oxidative process. According to previous

**Figure 3.** IR spectra of 10% ribose/SiO₂ activated under vacuum up to 250 °C.**Scheme 3.** A three-step mechanism leading to the formation of ribonolactone from D-ribose (see text).

reports,^[22] a three-steps mechanism is involved as illustrated in Scheme 3: A) formation of linear ribose (already illustrated in Scheme 2); B) oxidation of the carbonyl group to ribonic acid; and C) dehydration to ribonolactone.

To confirm the hypothesis that an oxidative process is taking place as postulated in Step B, thermal activation of ribose/SiO₂ was carried out in O₂ flow and the vibrational bands that we had assigned to linear ribose and to ribonolactone were quantified. The band of ribonolactone was five times more intense at 250 °C under O₂ flow than under (nominal) vacuum. At the same time, the proportion of linear ribose was twice as high under O₂ flow as under vacuum: the opening of the ribose ring seems also to be facilitated under O₂. The occurrence of an oxidative reaction under nominal vacuum remains surpris-

ing because our systems are not supposed to contain oxidants. The most logical candidate would be residual O_2 in the vacuum ramp. Attempts to duplicate our results revealed that the intensity of the band assigned to ribonolactone was indeed strongly dependent on the experimental setting.

With respect to the effect of ribose loading, the amount of linear ribose formed at a given temperature increases faster than the initial amount of ribose (Figure SI-2). This could hint at a chemical heterogeneity of the ribose/surface interaction. As for the amount of ribonolactone, it does not show a clear trend as a function of ribose coverage.

Effect of the coadsorption of divalent cation salts on the reactivity of adsorbed ribose

XRD and TGA

In ribose-Sr/SiO₂, XRD analysis revealed the presence of bulk SrCl₂. No bulk salt phases were observed for the other ribose-metal/SiO₂ samples. This probably means that metal cations (and chloride anions as well!) are well dispersed on the silica surface (see Figure SI-3 for X-ray diffractograms of the various samples).

DTG traces of the various ribose-metal/SiO₂ samples are presented in Figure 4 and the weight losses corresponding to the identifiable thermal events can be found in Table 2.

Most of the ribose-metal/SiO₂ samples, except ribose-Fe^{x+}/SiO₂, have similar TGA profiles, with three peaks in the DTG.

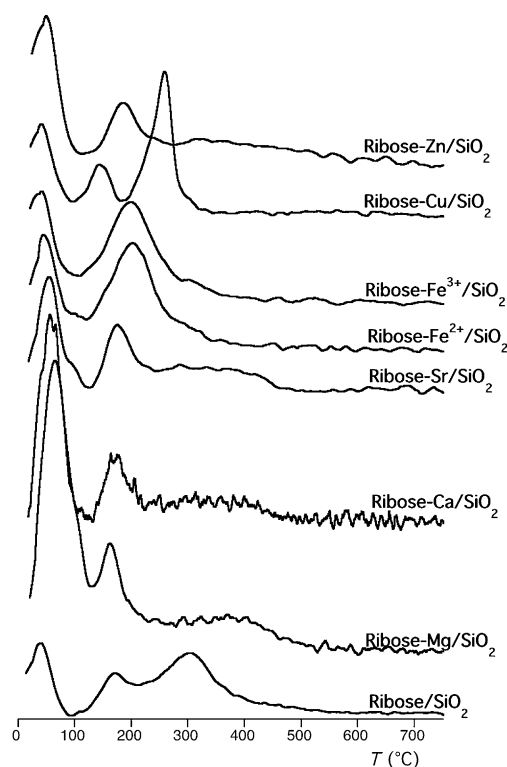


Figure 4. DTG traces of ribose-metal/SiO₂ samples

Table 2. Weight losses (in weight% of the silica support) corresponding to DTG peaks in ribose-metal/SiO₂ samples.

Sample	Peak Temp. T_{max} [°C]	Weight losses [%]	Thermal effect (DTA)	Total weight loss all ribose peaks [%]
ribose/silice	38	2.0	endothermic	9.8
	170	2.5	endothermic	
	304	7.3	exothermic	
ribose-Mg/SiO ₂	65	14.0	endothermic	12.3
	165	5.5	endothermic	
	~370	6.8	(weak)	
ribose-Ca/SiO ₂	57	6.4	endothermic	7.9
	172	3.4	endothermic	
	~320	4.5	exothermic	
ribose-Sr/SiO ₂	53	3.3	endothermic	9.6
	172	4.4	endothermic	
	~315	5.2	(weak)	
ribose-Fe ²⁺ /SiO ₂	42	3.9	endothermic	10.6
	200	10.6	exothermic	
ribose-Fe ³⁺ /SiO ₂	39	3.0	endothermic	9.6
	199	9.6	exothermic	
ribose-Cu/SiO ₂	43	1.8	endothermic	9.4
	144	2.6	?	
	257	6.8	(weak)	
ribose-Zn/SiO ₂	47	4.1	endothermic	11.1
	183	5.0	endothermic	
	320	6.1	exothermic	

The first peak under 100 °C is endothermic, the second between 150 and 200 °C is generally also endothermic (the direction of the effect is unclear in the case of ribose-Cu/SiO₂), and the third peak is exothermic when the thermal effect can be ascertained. Furthermore, the sum of the weight losses for the second and third peak is close to 10% for a majority of the samples (10 ± 0.6%), that is, close to the theoretical ribose loading, and it seems logical therefore to assign both of them to the elimination of ribose; note however that significantly higher values are measured for ribose-Zn/SiO₂ (11.1%) and ribose-Mg/SiO₂ (12.3%), and a significantly lower value for ribose-Cu/SiO₂ (7.9%).

The first peak below 100 °C can be attributed to the loss of weakly held water, which may be adsorbed on the free surface, interacting with ribose or bound to the cations (in their hydration sphere). It is also present in ribose-free metal salt/SiO₂ samples that were investigated separately (see Figure SI-4). In both Mg/SiO₂ and Cu/SiO₂, the shape of the peak shows a structure that probably indicates well-defined transitions between $[M(H_2O)_6]^{2+}$ complexes of well-defined stoichiometry. Generally speaking, it is difficult to discriminate between metal-bound and surface-bound water. However, the alkaline earth/SiO₂ series shows a strong variation in the amount of weight loss that follows the trend in hydrophilicity, with ribose-Mg/SiO₂ (17%) > ribose-Ca/SiO₂ (7.2%) > ribose-Sr/SiO₂ (6.45%), whereas transition-metal/SiO₂ samples contain lower amounts of water (5.0 to 5.5%).

Among the ribose-metal/SiO₂ samples, weight losses are also strongly variable. In ribose-alkaline earth/SiO₂ samples, they are very similar to the ribose-free samples, suggesting that hydration water mostly interacts with the metal cations and that this interaction is not disturbed by the presence of

ribose. On the other hand, in ribose-transition metal/SiO₂ samples, the presence of ribose does cause some changes in hydration, with ribose-Cu/SiO₂ being the least hydrated.

The second, endothermic peak in DTG traces is reminiscent of the peak that was observed at 170 °C in ribose/SiO₂, with a 2.5% weight loss. Note first that the metal salts themselves do not give rise to a TG event in this temperature range (Figure SI-4; CuCl₂/SiO₂ is an exception, with a small peak at 287 °C that may be due to a redox between chloride ions and Cu²⁺). In the presence of alkaline earth metals, the second peak is also located at 170 °C with a larger weight loss that depends on the nature of the metal cation: about 3.4, 5.5, and 4.4%, respectively, in the presence of calcium, magnesium, and strontium. Transition metals induce different changes. In the presence of copper, this peak shifts to a lower temperature (144 °C) with a 2.5% weight loss. In contrast, in the presence of zinc, this peak shifts to a higher temperature (185 °C) with a 4.1% weight loss. Some of the weight loss values seem too high to be assigned only to ribose dehydration reactions, because even extensive dehydration to furfural (see IR results and discussion) would result in the loss of only three water molecules per ribose; that is, a loss of 3.6% on the basis of a 10% ribose loading. Thus, some metal ions promote extensive ribose degradation at low temperatures.

The highest temperature peak observed in the thermograms shows an exothermic event that can be attributed to the oxidation of residual organic matter. In comparison to ribose/SiO₂ (where $T_{\text{max}} = 304$ °C), this peak is considerably broadened and shifted to higher temperatures in ribose-alkaline earth metals/SiO₂ systems (T_{max} between 315 and 370 °C) and ribose-Zn/SiO₂ (T_{max} about 320°). In contrast, the combustion of organic matter occurs at lower temperatures for ribose-Cu/SiO₂ ($T_{\text{max}} = 257$ °C) and even more so for ribose-Fe^{x+}/SiO₂, for which the combustion event cannot be separated from the second peak. In the latter two cases, the low-temperature combustion event suggests that the supported metal ion is intimately involved in the oxidation event.

FTIR spectroscopy

Room temperature spectra: The metal ions we investigated show different effects on the IR spectrum, both at room temperature and upon thermal activation. The spectra of the different samples are presented in Figure 5 and Figure 6.

Before thermal activation, differences with ribose/SiO₂ are already apparent (compare lowest spectra in Figure 5 and Figure 6 with Figure 3). The δ_{HOH} band of water around 1630 cm⁻¹ is a good indicator of the hydration state of the material. It is more intense in all ribose-metal/SiO₂ than in metal-free samples, and for the alkaline earth cations its intensity follows the order of hydrophilicity ($\text{Mg}^{2+} \gg \text{Ca}^{2+} > \text{Sr}^{2+}$), indicating that a lot of water is bound to the cations at room temperature. For the transition-metal cations, the order of intensity is ($\text{Fe}^{x+} \gg \text{Cu}^{2+} = \text{Zn}^{2+}$); however, the maximum intensity for the ribose-Fe/SiO₂ samples is artificially inflated by the presence of another band in close vicinity.

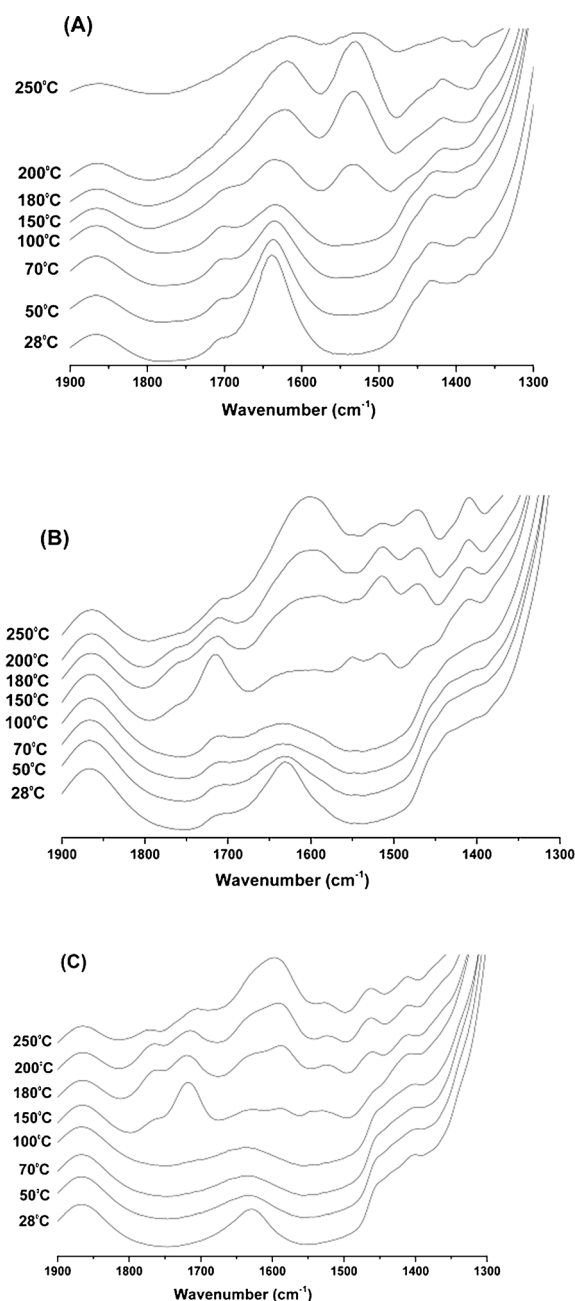


Figure 5. IR spectra as a function of activation temperature of ribose-Mg/SiO₂ (A), ribose-Ca/SiO₂ (B), and ribose-Sr/SiO₂ (C), with (1:1) molar equivalent.

As regards the δ_{HCH} vibrations, in ribose-transition metal/SiO₂, the band at 1452 cm⁻¹ is unaffected by the presence of the cations, whereas the second band shows significant bathochromic (red) shifts. We evaluate them at -20, -18, and -13 cm⁻¹, respectively, in ribose-Zn/SiO₂, ribose-Fe^{x+}/SiO₂, and ribose-Cu/SiO₂, for a ribose/metal molar ratio of 1:1, but it is less important in the ribose-metal (2:1)/SiO₂ series (ca. 8 cm⁻¹). This indicates a direct interaction between metals and sugar, probably involving the C5 carbon. The effect of alkaline earth cations on this band are more complex: it appears split into two components, one blueshifted and the second redshifted,

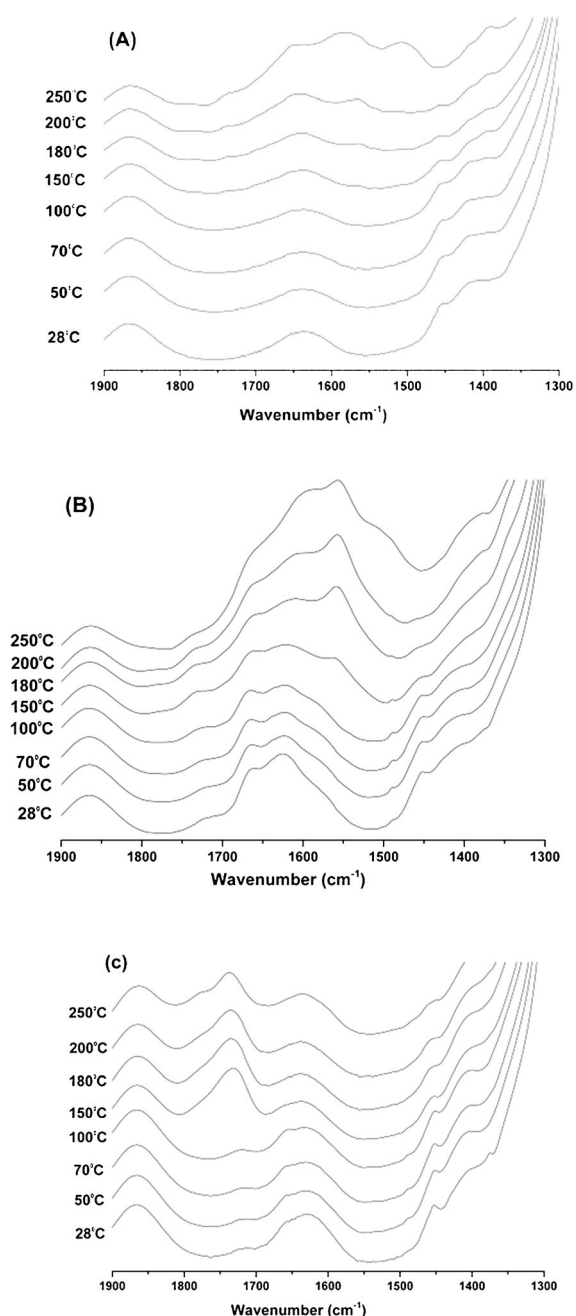


Figure 6. IR spectra as a function of activation temperature of ribose-Zn/SiO₂ (A), ribose-Fe/SiO₂ (B), and ribose-Cu/SiO₂ (C), with (1:1) molar equivalent.

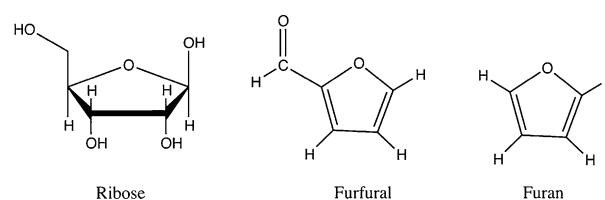
in ribose-Mg/SiO₂ and ribose-Sr/SiO₂, whereas only the blue-shifted component appears in ribose-Ca/SiO₂.

New bands are also apparent in the carbonyl stretching ($\nu_{C=O}$) region in ribose-Fe^{x+}/SiO₂ and ribose-Cu/SiO₂, for both molar ratios, but not in ribose-Zn/SiO₂. The first region, at 1714 cm⁻¹, appears for ribose-Cu/SiO₂ and ribose-Fe²⁺/SiO₂ (but not ribose-Fe³⁺/SiO₂). The similarity with the aldehyde band of furfural is probably coincidental because the other bands of this molecule are not present. We tentatively attribute the band at 1714 cm⁻¹ to a linear ribose; however, given that its wavenumber is significantly lower than in free linear ribose, we suggest that it corresponds to linear ribose complexed by iron(II).

The shoulder at 1661–1662 cm⁻¹ in ribose-Fe^{x+}/SiO₂ and 1658 cm⁻¹ in ribose-Cu/SiO₂ is probably characteristic of the enediol. The position of this band would then be significantly blueshifted with respect to the same species in bulk ribose, and this might be the effect of complexation to the metal ions. Enediols, like aromatic diols such as catechol or dopamine, are known to be good complexing agents,^[23] including for Fe^{x+} centers. The complexes of enediol with iron and copper ions could be stabilized by crystal field stabilization energy (CFSE) effects, causing a shift of the ribose isomerization equilibria towards this form.

With regard to the alkaline-earth-containing samples, a small band is observed at 1702 cm⁻¹ for ribose-Mg/SiO₂ and 1710–1715 cm⁻¹ for ribose-Ca/SiO₂, but it is not present for ribose-Sr/SiO₂. An assignment to complexed linear ribose may also be proposed here on the basis of parsimony, but the carbonyl shift would be more important in ribose-Mg/SiO₂ than in the other samples, which is somewhat surprising.

Effect of thermal activation on spectra: We shall now consider the evolution of IR spectra upon thermal activation. In ribose-Mg (1:1)/SiO₂, no changes are observed from room temperature to 100 °C, except for a gradual decrease of the band at 1630 cm⁻¹ indicative of dehydration. At 150 °C, a conspicuous new band appears at 1533 cm⁻¹ ($\nu_{C=C}$ region), which is a region in which no signal was detected for ribose/SiO₂ irrespective of the temperature. At the same time, an absorption in the 1400–1500 cm⁻¹ region was also modified with the appearance of a new maximum at 1415 cm⁻¹, and the carbonyl band was redshifted by -4 cm⁻¹; it seems to disappear above 180 °C. These observations suggest that ribose has been strongly dehydrated, with the concomitant production of C=C double bonds. One logical outcome of this dehydration reaction would be the formation of furfural (cf. Scheme 4), but this



Scheme 4. Furfural and furan, compared with D-ribose.

product should have a very strong $\nu_{C=O}$ band at 1714 cm⁻¹ because of its aldehyde function, which is not observed here. The product that forms must therefore have C=C double bonds and no aldehyde function. This is the case for furan, C₄H₄O, and the subtraction spectrum is indeed rather compatible with that of furan.^[24] The evolution of ribose-Mg (2:1)/SiO₂ is almost indiscernible from that of ribose-Mg (1:1)/SiO₂.

For ribose-Ca/SiO₂ and ribose-Sr/SiO₂, more complex changes are observed, with no less than six new bands appearing at 150 °C and above (1764, 1714–1718, 1580, 1538, 1475, and 1411 cm⁻¹). They correspond to several different products because their relative intensities change with the temperature.

One of the products could be ribonolactone ($\nu_{C=O}$ at 1764 cm^{-1}), which remains a minor species. The two bands in the $1500\text{--}1600\text{ cm}^{-1}$ range can be assigned, as above, to $\nu_{C=C}$ bands, possibly of different products. They appear at the same time as the $\nu_{C=O}$ at $1714\text{--}1718\text{ cm}^{-1}$ and together, these observations could indicate the formation of furfural. In comparison to ribose-Mg/SiO₂, we propose that in ribose-Ca/SiO₂ and ribose-Sr/SiO₂ both furfural (completely dehydrated product) and furan (dehydrated and decarboxylated) are formed.

Heating of ribose-Zn/SiO₂ to 150°C does not cause any changes in the spectrum. The first modifications are only apparent at 180° and become conspicuous at 200°C . They are very similar to what was observed at lower temperatures in ribose-Mg/SiO₂ and ribose probably undergoes the same transformations here, only at a significantly higher temperature. Thus, the presence of Zn²⁺ in a 1:1 ratio causes a thermal stabilization of ribose as compared with ribose/SiO₂, and, actually, also to the other ribose-metal/SiO₂. In contrast, the bands that we have previously assigned to linear ribose (1730 cm^{-1}) and ribonolactone (1780 cm^{-1}) are observed in ribose-Zn (2:1)/SiO₂ already at 150°C . We hypothesize that Zn²⁺ is able to form a complex with cyclic ribose that results in the stabilization of the latter molecule with respect to ring opening. If the stoichiometry of this complex is 1:1, then all ribose molecules may be complexed, and thus stabilized, in ribose-Zn (1:1)/SiO₂, whereas half of them would remain uncomplexed in ribose-Zn (2:1)/SiO₂, and therefore follow the same transformation as without zinc.

Copper and iron induce very different thermal reactivities compared with zinc and alkaline earths. Below 150°C , linear ribose (1720 cm^{-1}) and enediol (1658 cm^{-1}) are present, the latter in large quantities, in ribose-Cu/SiO₂ and ribose-Fe^{x+}/SiO₂.

In ribose-Cu/SiO₂, at 150°C , a very strong band grows in the $\nu_{C=O}$ region at 1731 cm^{-1} and the enediol band disappears. No bands are apparent in the $\nu_{C=C}$ region (this is in exact opposition to ribose-Mg/SiO₂). Several assignments could be proposed for this $\nu_{C=O}$ band. It might be due to one or several aldehydes, including glycolaldehyde,^[25] formed by catalytic retro-aldol fragmentation of ribose.^[26] Or it might be due to a carboxylic acid formed through the oxidation of ribose by Cu²⁺, which would then be acting as a stoichiometric reagent. Given that the amount of the corresponding product, as indicated by the relative band intensity, is about twice lower in ribose-Cu (2:1)/SiO₂ than in ribose-Cu (1:1)/SiO₂, we would favor the second interpretation, but clearly more work ought to be done to clarify this point. Local browning of the sample was observed, possibly due to the products of copper reduction.

In ribose-Fe/SiO₂ samples the reactivity seems different again. The complexed enediol form is preserved at high temperatures, whereas a new, sharp band appears at 1558 cm^{-1} and shoulders at 1510 and 1490 cm^{-1} at higher temperatures. Thus, here, dehydration reactions must be considered again. We will not endeavor to precisely identify the reaction product(s) formed in these samples because their nature is not

central to the main question motivating the present study, namely, the stability of ribose.

NMR spectroscopy

The ¹³C NMR spectrum of ribose in water solution has been reported previously and can be used as a basis for peak assignments in other samples. The spectrum we obtained (Figure SI-5) was identical to that published by Ortiz et al.^[27] In general, four signals can be observed for each carbon, corresponding to the four anomers (although there is some overlap); the α_p and β_p forms are more difficult to discriminate than the others. The C1 peaks are particularly well resolved and can be used to quantify the anomeric ratios; it can also be verified that very similar ratios are obtained on the basis of the C4 peaks.

We have also recorded liquid-state ¹³C NMR spectra of solutions containing ribose and metal chlorides (1:1 ratio) to assess the complexing power of these salts (Figure SI-6, and Table SI-2). The addition of MgCl₂, CaCl₂, or ZnCl₂ did not have much effect on the chemical shifts of the various peaks, with displacements in general smaller than 0.1 ppm (except for the C5 peaks for which +0.2 and +0.35 ppm shifts were observed in two cases). The intensity ratios were not significantly altered either. In contrast, the addition of SrCl₂ caused shifts up to 1.0 ppm, making the assignments of some peaks difficult, and the contribution of the α_f anomeric form was significantly exalted. In summary, the modifications of the ¹³C NMR spectra are very minor and do not indicate coordination of ribose to Mg²⁺, Ca²⁺, or Zn²⁺ in aqueous solution (nor any strong binding of ribose to Cl⁻); at most, the results indicate the possible formation of weakly H-bonded adducts. Sr²⁺ is a possible exception. These conclusions are significantly different from those of Ortiz et al.^[27] who observed more significant peak shifts (a few tenths to 2.0 ppm) for ribose in aqueous solution when KCl and NaCl were added to the medium; it should be noted, however, that these authors used much higher salt concentrations.

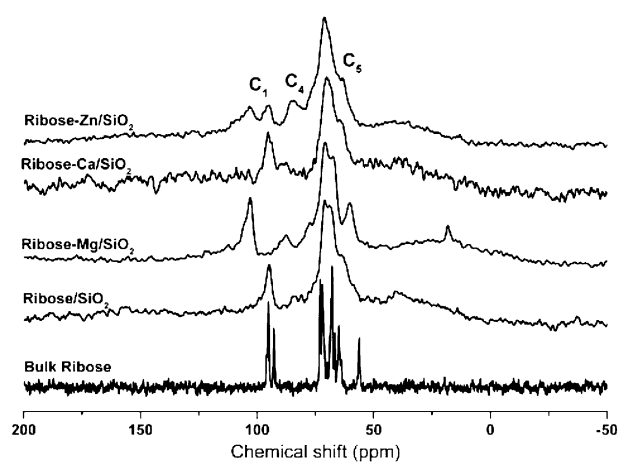


Figure 7. ¹³C NMR spectra of bulk ribose, ribose/SiO₂, and ribose-diamagnetic Metal/SiO₂ systems

The ^{13}C CP-MAS NMR spectra of ribose/ SiO_2 , ribose-Mg/ SiO_2 , ribose-Ca/ SiO_2 , and ribose-Zn/ SiO_2 are presented in Figure 7 and compared with that of bulk ribose.

Ribose interaction with the silica surface in the absence of cations has been discussed in a previous paper.^[14] In solution, the pyranose forms are predominant (82% of the total, for 18% of furanose forms). After adsorption on the silica surface, the NMR peaks are much broader, which is typical of solid-state NMR analysis, for where the molecules have a low mobility. NMR peak positions remain compatible with the chemical shifts of ribose carbon signals. Thus, only ribose is present on the silica surface, in its four anomeric forms; yet adsorption somewhat modifies the anomeric equilibria, as the furanose forms increase to about 25%, specifically due to promotion of the α_f form.

Likewise, for the ribose-metal/ SiO_2 samples, all individually resolved peaks may be assigned to ribose carbon atoms, and the remaining part of the spectrum is compatible with the envelope of overlapping ribose peaks. Table S11 summarizes the chemical shifts of the various samples, at least those that could be determined precisely. Important shifts are observed in some cases with respect to ribose in solution, especially for ribose-Mg/ SiO_2 for which the peaks corresponding to C1 are shifted between -3.6 and $+7.2$ ppm, whereas those of C4 and C5 are affected to a lesser extent; all the enantiomers are affected. In ribose-Ca/ SiO_2 , in contrast, the peaks of C4 and C5 undergo more significant shifts than those of C1.

In ribose-Zn/ SiO_2 , among the signals that can be clearly discriminated, the C1 peaks of the two furanose isomers are strongly affected, their C2 and C4 peaks much less so. The C1 peaks of the pyranose forms are also shifted, but the effect is three times smaller than for the furanoses, leading us to believe that the latter are more strongly complexed.

Quantification of the anomeric forms was carried out on the basis of the C1 peaks, which are the best resolved; the results are reported in Table 3. In some samples the C4 peaks were sufficiently well-resolved to provide an independent estimate of the enantiomeric ratios, and these estimates were not significantly different from the C1-based ratios.

Coadsorption with metallic salts promotes the ribofuranose forms over the ribopyranoses, as did the adsorption on bare silica, but to a larger extent. The proportion of ribofuranoses increases from 24% in ribose/ SiO_2 to 34, 51, and 64%, respectively, in ribose-Mg/ SiO_2 , ribose-Ca/ SiO_2 , and ribose-Zn/ SiO_2 . The β/α ratios are also affected. In ribose-Mg/ SiO_2 and ribose-

Ca/ SiO_2 , both anomeric forms of ribofuranose increase, but the α_f to a larger extent than the β_f , leading to a β/α ratio of 0.8 and 0.7, respectively, as compared with 1.6 in ribose/ SiO_2 . In contrast, the opposite trend is observed in ribose-Zn/ SiO_2 : the β/α ratio actually increases to 3.6.

General Discussion

Some articles concerning amino acids have drawn attention to the prebiotic potential of bulk organic molecules,^[28] and therefore the study of bulk ribose is relevant. Our initial study of the reactivity of bulk ribose can be used as a benchmark against which to evaluate the stability of ribose molecules in other environments. Melting at 90°C already induces chemical heterogeneity, as indicated by the IR study and by simple visual inspection. The inception of some chemical transformations depends on the heating procedure. One particular transformation that is easy to demonstrate spectroscopically is ring opening to linear ribose, followed by isomerization to enediol. Flash heating induces ring opening already at 90°C , and even upon gentle heating these reactions clearly appear at 150°C . It can be said with confidence that bulk ribose is no longer stable at 150°C .

When ribose is deposited on SiO_2 , it remains in the form of a cyclic monomer. In particular, there are no observations that might indicate polymerization, probably due to the restriction in molecular mobility upon adsorption that prevents the monomers from encountering each other. The only effect of adsorption on ribose speciation is modification of the anomeric equilibria, as discussed below. At 150°C and above, ribose undergoes ring opening; between 180 and 200°C , oxidation must occur because a minor amount of ribonolactone is formed. The most likely oxidant is adventitious dioxygen remaining in the vacuum ramp (and if it is the case, the corresponding reaction would not be of prebiotic significance because the primordial atmosphere of the Earth was anoxic). Another possibility would be adsorbed water; although normally a weak oxidant, its reaction could be enhanced by removal of its reduction product, that is, H_2 , under vacuum. However, we did not observe any H_2 formation, and, moreover, the remaining amount of adsorbed water at 180°C is certainly quite small; therefore we do not favor this possibility. At 250°C , not much organic matter remains on the surface. Also interesting is what is *not* observed on silica: there is no evidence of the formation of unsaturated compounds with $\text{C}=\text{C}$ double bonds that would be formed by dehydration of ribose. Now the silica surface is moderately acidic (with about 4.5 Si-OH surface groups per nm^2 , of varying Brønsted acidity). Under anhydrous conditions and with the possibility of acid catalysis, ribose could evolve all the way to furfural (a reaction, accompanied by the loss of three water molecules per ribose, that was evidenced as early as 1943^[29]), or stop at an intermediate dehydration step. In fact, investigations on the dehydration of the closely related xylose molecule have shown that the Brønsted acidic centers of silica were much less active than the Lewis acidic centers of silico-aluminas.^[30] Nevertheless, the well-defined thermal event at 150°C in TG suggests that ribose

Table 3. Anomeric ratios calculated on the basis of the intensity of the C1 peaks.

Sample	α_p [%]	β_p [%]	Total pyranose	α_f [%]	β_f [%]	Total furanose
Ribose solution	20	62	82	6	12	18
Solid ribose	n.d.	n.d.	100	–	–	0
ribose/ SiO_2	29	47	76	15	9	24
ribose-Mg/ SiO_2	18	48	66	18	16	34
ribose-Ca/ SiO_2	23	26	49	29	22	51
ribose-Zn/ SiO_2	27	9	36	14	50	64

dehydration does occur in ribose/SiO₂. It is possible that the dehydration products do not stay on the surface and are quickly desorbed under the conditions of IR analysis (vacuum), whereas they burn in the air flow of the TG analysis.

In summary, cyclic ribose adsorbed on silica is stable up to about 150 °C; this sets an upper limit on the conditions under which prebiotic scenarios involving this molecule could be invoked.

Divalent metal salts can definitely interact with ribose in a specific way. The interaction is minimal in aqueous solution, at least for the concentration we investigated: according to liquid-state ¹³C NMR spectroscopic analysis, only very weak, outer-sphere interactions are established between ribose and metal salts (with the possible, and quite unexpected, exception of Sr²⁺). The metal cations must be present as aqua complexes, and remain so as long as the water activity is high enough. As soon as drying removes water ligands, these cations establish rather strong interactions with ribose and may already cause significant transformations at the low temperature of 70 °C. It is all but certain that every cation we tested is able to form specific complexes with ribose upon co-adsorption on silica. This is indicated by IR spectroscopic analysis, for which the δ_{HCH} shifts betray a strong interaction of the C5 carbon with the metal through its C-O-H moiety. IR analysis cannot be used to determine whether the other carbon atoms are involved in the interaction (at least not in the wavenumber range accessible under our experimental conditions), but solid-state ¹³C NMR spectroscopic analysis clearly shows strong shifts of at least some of the other carbon signals, and we may conclude that ribose acts as a polydentate ligand. Establishing the precise stoichiometry and molecular structure of the resulting complexes goes beyond the aims of the present article and would require much additional work. In the solid state, some cations such as Ca²⁺ form 1-D coordination polymers with pentoses,^[31] but in view of the submonolayer density of ribose in our samples this does not seem likely, and the complexes formed on silica may have original structures.

The enantiomeric distribution of ribose in our samples is also interesting. In a previous communication, we noted that the furanose isomers were more prominent in ribose/SiO₂ than in water solution.^[14] The tendency toward furanose stabilization is stronger in ribose-Mg/SiO₂ and ribose-Ca/SiO₂ (for which they respectively account for 34 and 51% of total ribose, compared with 24%). It is even more pronounced in ribose-Zn/SiO₂, with 64% of furanose isomers, but this sample is unique in favoring the β over the α isomer, whereas the opposite effect is observed with the other cations. The predominance of furanose is interesting because RNA exclusively uses a furanose form of ribose, which is not the predominant isomer in pure water solution.

The evolution of the anomeric ratio has been studied in the presence of borate^[8a,32] and silicate^[8c,33] anions. In both cases, the use of borate or silicate during the formose reaction stabilized ribose, and, more specifically, its furanose forms. Ribose speciation evolved even more by association of borate and alkali or alkaline earth cations.^[32a] The best result obtained was for the association of potassium and borate, which led to the

formation of only furanose isomers. Nevertheless, the use of borate has been disputed. The emergence of life probably occurred around 3.7 Ga, but the oldest boron-containing mineral is probably only 3.6 Ga old.^[34] Moreover, borates were probably not in sufficiently high concentration to be used in chemical reactions or to precipitate to allow prebiotic reactions at the interface.

The question of ribose anomeric speciation goes beyond furanose vs. pyranose. Today's RNA is more specifically constituted of the β -D-ribofuranose isomer and therefore the α vs. β distribution of ribose is also relevant. Recently, Singh et al.^[35] studied the glycosylation of adenine in water/acetonitrile mixtures. They observed the preferential formation of a β -nucleotide and tried to rationalize this observation in a mechanism involving a nucleophilic attack of the adenine base on ribose with inversion of configuration, making the hypothesis that the approach of the nucleophilic base was favored by a specific pattern of H-bonding with the α_f ribose anomers. The details of the mechanism are likely to be different on the silica surface, and insufficient molecular information is available to speculate on this, but the special behavior of Zn chloride, which favors the β anomer, would be worth investigating in glycosylation experiments.

Co-adsorption of inorganic salts causes striking modifications of the thermal reactivity of adsorbed ribose. We do not believe that interaction with the anion is the main factor, given that we used the same compensating anion in all samples, and observed different behaviors depending on the nature of the cation. Already after drying at 70 °C ring opening is observed with Mg²⁺ and Ca²⁺. This isomerization to linear ribose could be catalyzed by coordination to the alkali metal cation. Beyond the reaction kinetics, the equilibrium (if it is indeed attained) does not favor the linear form, which remains a minority species and could not be separately observed by NMR spectroscopic analysis. Zn²⁺ and Sr²⁺ do not cause ring opening (see below for further discussion). Cu²⁺ and Fe^{x+} cause a more extensive transformation to the enediol form, probably because of their capacity to make coordination compounds with the latter.

Thermal activation under vacuum results, in most cases, in rather abrupt modifications of the IR spectrum at about 150 °C, as on bare silica. With alkaline earth metals, unsaturated products resulting from ribose dehydration appear. For ribose-Mg/SiO₂, only weak carbonyl signals are observed, suggesting that furfural, the end product of complete ribose dehydration (with a loss of three H₂O per ribose), is not predominant. A possible explanation would be that carbon centers in the furanose cycle are dehydrated first (with a loss of up to two H₂O per ribose), while keeping the -CH₂OH group intact. However, this does not correspond with known dehydration mechanisms,^[36] and besides TG shows that this sample loses more than two H₂O per ribose, not less, in the dehydration peak at 165 °C. We have mentioned that IR data are compatible with transformation of ribose into furan; the calculated weight loss would be 5.5% (reported to the mass of SiO₂), in keeping with its quantification in TG. Furan can be obtained from furfural by

decarbonylation, although the catalysis of this transformation usually involves transition metals.

In contrast, for ribose-Ca/SiO₂ and ribose-Sr/SiO₂, a strong carbonyl peak appears at 1714–1716 cm⁻¹ at the same time as the C=C bands, consistent with the formation of furfural. The latter molecule would coexist with furan, because the experimental weight losses fall between the theoretical values corresponding to furfural formation (–3.2% expected weight loss) and furan formation (–5.5%), while a minor amount of ribonolactone would be formed in a side reaction. The formation of furfural deserves some comments. Obtaining furfural from D-xylose (a pentose rather similar to D-ribose, itself derived from the hydrolysis of hemicellulose) is a challenge in green chemistry. This reaction is usually carried out in slurries, and the effect of metal salt additives has been studied in some depth. An undesirable side reaction is the formation of polymeric humins from furfural condensation.^[37] In our samples, when furfural is formed, it does not polymerize because of its limited mobility on the silica surface, and therefore catalytic systems based on CaCl₂/SiO₂ or SrCl₂/SiO₂ could perhaps be applied for the industrial synthesis of furfural. At any rate, mechanistic insights gained on xylose transformation may also prove useful to understand ribose transformation,^[37–38] even though the experiments are carried out in quite different environments (concentrated slurries instead of solid-vacuum interface). In particular, Enslow et al.^[37] have proposed that ribose complexation through its C-OH groups can weaken the C–O bonds and thus facilitate dehydration, in a type of Lewis acid catalysis.

Ribose-Zn/SiO₂ undergoes the same transformations as ribose-Mg/SiO₂, but at a considerably higher temperature: cyclic ribose is intact at 150 °C, it starts transforming into dehydration products at 180 °C, and is extensively transformed, probably into furan, only at 200 °C (this is compatible with *T*_{max} and weight loss observed in TG). Thus, from the point of view of ribose stabilization that was the driving force of the present study, co-adsorption with Zn²⁺ on silica is the most efficient treatment. It is crucial that Zn²⁺ prevents ring opening to linear ribose, because the formation of the latter intermediate, followed by isomerization to enediol, can easily result in further reactions, for example, to ribulose, arabinose, and thus presumably to loss of (pre)biological selectivity.

In the presence of copper (Cu²⁺), ribose transformation follows a different path. As mentioned above, the ν_{C=C} indicative of dehydration is not observed but a strong ν_{C=O} band appears. The weight loss is smaller than for all other cations tested and occurs at a lower temperature. The reaction that occurs could be a partial oxidation of the ribose skeleton. Although a minor amount of ribose can be oxidized by residual O₂ in the vacuum ramp, the phenomenon that occurs here is more extensive and it is possible that Cu²⁺ itself acts as an oxidizing agent, thus playing the role of a reagent and not of a catalyst.

Phenomena observed with iron (Fe²⁺ and Fe³⁺) are complex. As mentioned, they involve ring opening at low temperatures and probably dehydration reactions at 150 °C and higher under vacuum, without the formation of an aldehyde function. This reactivity is grossly similar to that observed with Mg²⁺, yet the product formed does not have exactly the same spec-

troscopic signature. Under TG conditions, i.e., under air flow, the reactivity seems noticeably different from vacuum conditions, in contrast to what is observed for the other systems: all the adsorbed ribose is removed in an exothermal reaction taking place at 200 °C, meaning that the Fe^{x+} ions catalyze the combustion of ribose by dioxygen in the air. From a prebiotic point of view, this is less relevant than the reactivity under vacuum.

Conclusion

With respect to bulk ribose, and even more to ribose in aqueous solutions, adsorption on silica results in stabilization of the cyclic molecules up to about 150 °C, thus extending the useful “temperature window” for prebiotic reactions by more than 50 °C; the anomeric speciation is only slightly modified with respect to the solution. At 150 °C, ring opening starts to occur, and this is a doorway to pentose isomerization and loss of chemical specificity.

The alkaline earth and transition metal salts investigated here (MgCl₂, CaCl₂, SrCl₂, CuCl₂, FeCl₂, FeCl₃, ZnCl₂) show little tendency to interact with ribose in solution. However, when they are deposited together with ribose on the silica surface and submitted to drying, they form coordination complexes in which ribose acts as a multidentate ligand. The detailed structures of these complexes have not yet been resolved. Complexation influences the anomeric ratios, with the most remarkable effect being observed for Zn²⁺, which favors the furanose forms and especially the β_f isomer.

The effects of inorganic salts on the thermal reactivity of ribose are very diverse depending on the chemical nature of the cations. Alkaline earth cations do not extend the temperature stability of ribose with respect to the salt-free system, and, in fact, they cause a minor amount of ring opening already at low temperature. At 150 °C and above, they catalyze ribose dehydration leading to furfural and also, to variable extents, decarbonylation of the latter to furan. These reactions probably follow a Lewis acidic catalytic mechanism, and might be useful for the valorization of biomass-derived products.

Copper and iron ions cause a more extensive ring opening and isomerization at low temperature (to the enediol form). At higher temperatures, they initiate complicated reactions in which their ability to take part in redox reactions, either as reagents or as catalysts, plays a role together with their Lewis acid catalytic properties. They certainly do not look promising to stabilize ribose at high temperatures.

In this respect, zinc appears unique because it preserves cyclic ribose at least up to 180 °C. Although the present work may have applications other than in prebiotic chemistry, from the latter point of view, it will be interesting to study the reactivity of ribose-Zn/SiO₂ systems in further reactions that might lead to RNA, namely glycosylation and phosphorylation processes.

Acknowledgements

Mariame Akouche was supported by a Ph.D. grant from the Ile-de-France region, under the DIM-ACAV program. The SESAME program of the French Ile de France Region is acknowledged for financial support for the purchase of the 500 MHz NMR spectrometer.

Keywords: heterogeneous catalysis • RNA • silicon • surface analysis • surface chemistry

- [1] W. Gilbert, *Nature* **1986**, 319, 618.
- [2] S. A. Benner, H.-J. Kim, M. A. Carrigan, *Acc. Chem. Res.* **2012**, 45, 2025–2034.
- [3] C. Meinert, I. Myrgorodska, P. de Marcellus, T. Buhse, L. Nahon, S. V. Hoffmann, L. Le Sergeant d'Hendecourt, U. J. Meierhenrich, *Science* **2016**, 352, 208–212.
- [4] S. Becker, I. Thoma, A. Deutsch, T. Gehrke, P. Mayer, H. Zipse, T. Carell, *Science* **2016**, 352, 833–836.
- [5] R. Shapiro, *Orig. Life Evol. Biosph.* **1988**, 18, 71–85.
- [6] R. Larralde, M. P. Robertson, S. L. Miller, *Proc. Natl. Acad. Sci. USA* **1995**, 92, 8158–8160.
- [7] D. Sisak, L. B. McCusker, G. Zandomenighi, B. H. Meier, D. Bläser, R. Boese, W. B. Schweizer, R. Gilmour, J. D. Dunitz, *Angew. Chem.* **2010**, 49, 4503–4505.
- [8] a) A. Ricardo, M. A. Carrigan, A. N. Olcott, S. A. Benner, *Science* **2003**, 63, 96–96; b) H.-J. Kim, A. Ricardo, H. I. Illangkoon, M. J. Kim, M. A. Carrigan, F. Frye, S. A. Benner, *J. Am. Chem. Soc.* **2011**, 133, 9457–9468; c) J. B. Lambert, G. Lu, S. R. Singer, V. M. Kolb, *J. Am. Chem. Soc.* **2004**, 126, 9611–9625; d) A. Vázquez-Mayagoitia, S. R. Horton, B. G. Sumpter, J. Sponer, J. E. Sponer, M. Fuentes-Cabrera, *Astrobiology* **2011**, 11, 115–121.
- [9] D. Bernal, *The Physical Basis of Life*, Routledge and Kegan Paul, London, **1951**.
- [10] J.-F. Lambert, *Origins Life Evol. Biospheres* **2008**, 38, 211–242.
- [11] a) S. Balme, R. Guegan, J.-M. Janot, M. Lepoitevin, M. Jaber, P. Dejjardin, X. Bourrat, M. Motelica-Heino, *Soft Mater.* **2013**, 9, 3188–3196; b) M. Lepoitevin, M. Jaber, R. Guegan, J. M. Janot, P. Dejjardin, F. Henn, S. Balme, *Appl. Clay Sci.* **2014**, 95, 396–402.
- [12] J. P. Ferris, A. R. J. Hill, R. Liu, L. E. Orgel, *Nature* **1996**, 381, 59–61.
- [13] a) M. Meng, L. Stievano, J.-F. Lambert, *Langmuir* **2004**, 20, 914–923; b) L. Stievano, L. Piao, I. Lopes, M. Meng, D. Costa, J.-F. Lambert, *Eur. J. Mineral.* **2007**, 19, 321–331; c) I. Lopes, L. Piao, L. Stievano, J.-F. Lambert, *J. Phys. Chem. C* **2009**, 113, 18163–18172; d) J.-F. Lambert, L. Stievano, I. Lopes, M. Gharsallah, L. Piao, *Planet. Space Sci.* **2009**, 57, 460–467; e) M. Bouchoucha, M. Jaber, T. Onfroy, J.-F. Lambert, B. Xue, *J. Phys. Chem. C* **2011**, 115, 21813–21825; f) M. Jaber, J. Spadavecchia, H. Bazzi, T. Georgelin, F. Costa-Torro, J.-F. o. Lambert, *Amino Acids* **2013**, 45, 403–406; g) J.-F. Lambert, M. Jaber, T. Georgelin, L. Stievano, *Phys. Chem. Chem. Phys.* **2013**, 15, 13371–13380; h) T. Georgelin, M. Jaber, H. Bazzi, J.-F. Lambert, *Origins Life Evol. Biospheres* **2013**, 43, 429–443; i) T. Georgelin, M. Jaber, T. Onfroy, A.-A. Hargrove, F. Costa-Torro, J.-F. o. Lambert, *J. Phys. Chem. C* **2013**, 117, 12579–12590; j) M. Jaber, T. Georgelin, H. Bazzi, F. Costa-Torro, J.-F. Lambert, G. Bolbach, G. Clodic, *J. Phys. Chem. C* **2014**, 118, 25447–25455.
- [14] T. Georgelin, M. Jaber, F. Fournier, G. Laurent, F. Costa-Torro, M.-C. Maurel, J.-F. Lambert, *Carbohydr. Res.* **2015**, 402, 241–244.
- [15] a) A. Raemy, T. F. Schweizer, *J. Therm. Anal.* **1983**, 28, 95–108; b) P. Tomasiak, M. Palasinski, S. Wiejak, *Adv. Carbohydr. Chem. Biochem.* **1989**, 47, 203–278; c) Y. Roos, *Carbohydr. Res.* **1993**, 238, 39–48; d) M. Hurta, I. Pitkänen, J. Knuutinen, *Carbohydr. Res.* **2004**, 339, 2267–2273; e) S. T. Beckett, M. G. Francesconi, P. M. Geary, G. Mackenzie, A. P. E. Maulny, *Carbohydr. Res.* **2006**, 341, 2591–2599; f) A. Magon, M. Pyda, *Carbohydr. Res.* **2011**, 346, 2558–2566; g) J. W. Lee, L. C. Thomas, S. J. Schmidt, *J. Agric. Food Chem.* **2011**, 59, 684–701.
- [16] M. R. M. Izawa, H. W. Nesbitt, N. D. MacRae, E. L. Hoffman, *Earth Planet. Sci. Lett.* **2010**, 298, 443–449.
- [17] a) G. Wächtershäuser, *System. Appl. Microbiol.* **1988**, 10, 207–210; b) A. Y. Mulikdjanian, *Biol. Direct* **2009**, 4, 26.
- [18] a) M. C. Ramos-Sanchez, F. J. Rey, F. J. M.-G. M. L. Rodriguez-Mendez, J. Martin-Gil, *Thermochim. Acta* **1988**, 134, 55–60; b) U. Räisänen, I. Pitkänen, H. Halttunen, M. Hurta, *J. Therm. Anal. Calorim.* **2003**, 72, 481–488; c) M. Lappalainen, I. Pitkänen, H. Heikkilä, J. Nurmi, *J. Therm. Anal. Calorim.* **2006**, 84, 367–376.
- [19] M. A. Mathlouthi, A.-M. Seuvre, J. L. Koenig, *Carbohydr. Res.* **1983**, 122, 31–47.
- [20] V. A. Yaylayan, A. A. Ismail, *Carbohydr. Res.* **1992**, 11, 149–158.
- [21] L. T. Zhuravlev, *Colloids Surf. A* **2000**, 173, 1–38.
- [22] R. G. Compton, C. H. Bamford, C. F. H. Tipper, *Ester Formation and Hydrolysis and Related Reactions*, Elsevier, Amsterdam, **1972**.
- [23] T. Rajh, L. X. Chen, K. Lukas, T. Liu, M. C. Thurnauer, D. M. Tiede, *J. Phys. Chem. B* **2002**, 106, 10543–10552.
- [24] J. S. Kwiatkowski, J. Leszczynski, I. Teca, *J. Mol. Struct.* **1997**, 436–437, 451–480.
- [25] T. J. Johnson, R. L. Sams, L. T. M. Profeta, S. K. Akagi, I. R. Burling, R. J. Yonkelson, S. D. Williams, *J. Phys. Chem. A* **2013**, 117, 4096–4107.
- [26] M. S. Holm, Y. J. Pagán-Torres, S. Saravanamurugan, A. Riisager, J. A. Dumescic, E. Taarning, *Green Chem.* **2012**, 14, 702–706.
- [27] P. Ortiz, J. Fernández-Bertrán, E. Reguerac, *Spectrochim. Acta Part A* **2005**, 61, 1977–1983.
- [28] a) M. Rodríguez-García, A. J. Surman, G. J. T. Cooper, I. Suárez-Marina, Z. Hosni, M. P. Lee, L. Cronin, *Nature Com.* **2015**, 6, 8385; b) V. M. Kolb, *Int. J. Astrobiol.* **2012**, 11, 43–50.
- [29] R. C. Hockett, A. Guttag, M. E. Smith, *J. Am. Chem. Soc.* **1943**, 65, 1–3.
- [30] S. J. You, Y. T. Kim, E. D. Park, *React. Kinet. Mech. Cat.* **2014**, 111, 521–534.
- [31] C. B. Black, H.-W. Huang, J. A. Cowan, *Coord. Chem. Rev.* **1994**, 135/136, 165–202.
- [32] a) A. F. Amaral, M. Matild Marques, J. L. da Silva, J. J. R. Fraústo da Silva, *New J. Chem.* **2008**, 32, 2043–2049; b) Y. Furukawa, M. Horiuchi, T. Kakegawa, *Origins Life Evol. Biospheres* **2013**, 43, 353–361.
- [33] J. B. Lambert, S. A. Gurusamy-Thangavelu, K. Ma, *Science* **2010**, 327, 984–986.
- [34] R. M. Hazen, A. Bekker, D. L. Bish, W. Bleeker, R. T. Downs, J. Farquhar, J. M. Ferry, E. S. Grew, A. H. Knoll, D. Papineau, J. P. Ralph, D. Sverjensky, J. W. Valley, *Am. Mineral.* **2011**, 96, 953–963.
- [35] P. Singh, A. Singh, J. Kaura, W. Holzer, *RSC Adv.* **2014**, 4, 3158–3161.
- [36] M. Wang, C. Liu, Q. B. Li, X. X. Xu, *J. Mol. Model.* **2015**, 21, 296.
- [37] K. R. Enslow, A. T. Bell, *ChemCatChem* **2015**, 7, 479–489.
- [38] B. Danon, G. Marcotullio, W. de Jong, *Green Chem.* **2014**, 16, 39–54.

Received: March 25, 2016

Published online on ■■■■■, 0000

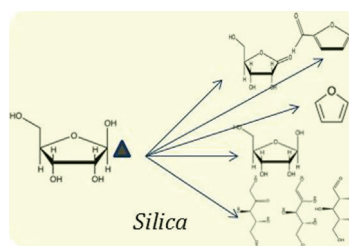
FULL PAPER

Prebiotic Chemistry

M. Akouche, M. Jaber, E.-L. Zins,
M.-C. Maurel, J.-F. Lambert,* T. Georgelin*



**Thermal Behavior of D-Ribose
Adsorbed on Silica: Effect of Inorganic
Salt Coadsorption and Significance for
Prebiotic Chemistry**



On silica chemistry: Ribose reactivity upon thermal activation when adsorbed on silica, either alone or with the coadsorption of inorganic salts, in the "RNA world" scenario is examined (see scheme). These results allow the likelihood of prebiotic chemistry scenarios to be evaluated, and may also be of interest for the valorization of biomass-derived carbohydrates by heterogeneous catalysis.